AEROACOUSTIC SIMULATION OF SOFT PHONATION EMPLOYING A KINEMATIC MODEL OF MUCOSAL WAVES

Jan Valášek[1,2], Anna Lancmanová[1], Prokop Pučejdl[1], Petr Sváček[1]

[1] *Department of Technical Mathematics, Faculty of Mechanical Engineering, Czech Technical University in Prague, Karlovo nám. 13, Praha 2, 121 35, Czech Republic*
[2] *Institute of Mathematics, Czech Academy of Sciences, Žitná 25, 115 67 Praha 1, Czech Republic*

Abstract

This work presents a hybrid computational framework for the simulation of human phonation, combining prescribed vocal fold motion, computational fluid dynamics, and aeroacoustic wave propagation. The airflow through the glottis is computed using an incompressible Navier–Stokes solver implemented in OpenFOAM, while acoustic propagation is modeled by the aeroacoustic wave equation (AWE). The approach avoids the complexity of fluid–structure interaction by prescribing physiologically relevant vocal fold kinematics, enabling controlled investigation of flow-induced sound generation. The influence of flow dynamics on acoustic source terms is analyzed, and numerical simulations of sound propagation in a simplified vocal tract geometry are presented.

Keywords: *human phonation, kinematic model of motion, AWE, FSI* ***FSI***.

1. Introduction

Human phonation is a multiphysics process involving interaction between airflow, vocal fold motion, and acoustic wave propagation. The dominant sound generation mechanism in normal speech is aerodynamic, arising from the unsteady airflow through the glottis [1].

Fully coupled fluid–structure–acoustic interaction (FSAI) models remain computationally demanding. Therefore, hybrid approaches are commonly employed, in which the flow field is computed using an a priori prescribed vocal fold motion rather than a fully coupled fluid–structure interaction simulation [2]. Besides significantly reducing computational cost, this simplification eliminates the need for structural modeling. The resulting flow field is subsequently used as input to an acoustic analogy, particularly such approach can be applied in the case of normal speech having relatively low acoustic pressure.

In this work, we adopt such a hybrid strategy. Instead of solving a fully coupled FSI problem, the vocal fold motion is prescribed using the kinematic model developed by Prof. Švec [3]. This allows for systematic investigation of aeroacoustic source mechanisms while reproducing physiologically realistic vocal fold kinematics.

2. Mathematical Model

The computational domain of flow problem Ω_t^f is based on the M5 benchmark model [4], see Fig. 1. This domain changes periodically in time to mimic vocal folds motion, which is realized by prescribed motion of interface boundary Γ_{W_t}, whereas the remaining boundaries $\partial\Omega_t^f \setminus \Gamma_{W_t}$ are static. Substantially larger acoustic domain Ω^a, see Fig. 2, is compoused of: the domain $\Omega_{\mathrm{ref}}^f = \Omega_{t=0}^f$, where the sound sources are computed, the domain Ω_{air}^a, which represents the vocal tract model and the far field region (outside of mouth), and the PML domain Ω_{pml}^a, where the perfectly matched layer (PML) technique is used to damp the outgoing acoustic waves, see [5].

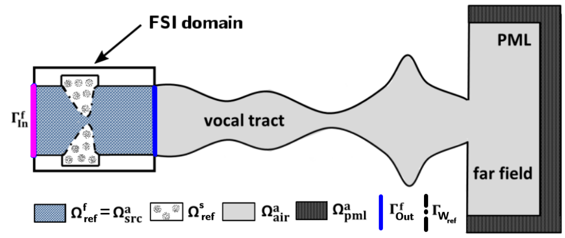

Figure 1: Schematic 2D cut in the middle of 3D geometrical FSAI domain in the reference configuration.

Corresponding author: *jan.valasek@fs.cvut.cz.*

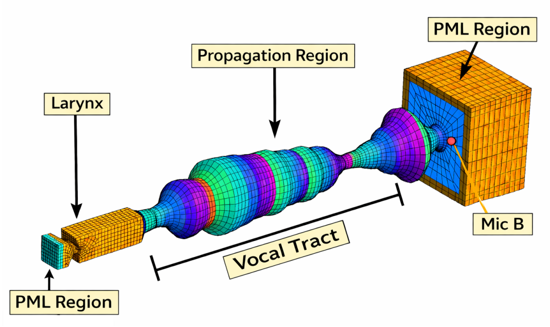

Figure 2: Acoustic 3D domain and its parts, which correspond to notation of Fig. 1.

2.1. Flow model

In order to include effects of domain change in time the ALE method is applied, [6]. Then airflow is described by the incompressible viscous Navier–Stokes equations in ALE formulation in Ω^f_{t} and $t \in (0, \mathrm{T})$

$$\frac{D^A \mathbf{v}}{Dt} + ((\mathbf{v} - \mathbf{w}_D) \cdot \nabla)\mathbf{v} + \nabla p = \nu^f_{\mathrm{eff}} \Delta \mathbf{v} = \mathbf{0}, \quad (1)$$

$$\mathrm{div}\ \mathbf{v} = 0, \quad (2)$$

where vector $\mathbf{v}(x,t)$ denotes the velocity, $p(x,t)$ the kinematic pressure and ν^f the kinematic viscosity. The symbol $\frac{D^A}{Dt}$ denotes the so called ALE derivative and vector $\mathbf{w}_D(x,t)$ is the ALE domain velocity. Further, ν^f_{eff} denotes the effective kinematic viscosity. For laminar flow, $\nu^f_{\mathrm{eff}} = \nu^f$, whereas in turbulent simulations it is augmented by the eddy viscosity,

$$\nu^f_{\mathrm{eff}} = \nu^f + \nu_t,$$

where ν_t is obtained from the selected turbulence model.

Here, we use the SST k–ω turbulence model as this model combines the advantages of the k–ω formulation in the near-wall region with the robustness of the k–ε model in the free stream. Thus it provides reliable prediction of separated flows and shear layers forming in the glottal jet.

The no-slip boundary condition $\mathbf{v}(x,t) = \mathbf{0}$ is given on channel walls and the velocity profile $\mathbf{v}(x,t) = \mathbf{v}_{\mathrm{in}}(x)$ is prescribed at the inlet, zero reference pressure is considered at the outlet and velocity continuity condition $\mathbf{v}(x,t) = \mathbf{w}_D(x,t)$ is prescribed on the moving interface $\Gamma^f_{\mathrm{W_t}}$ according to known kinamtic motion.

2.2. Prescribed vocal fold motion

We adopt the kinematic approach of [3], where the vocal fold (VF) motion is prescribed so as to reproduce essential features of phonation, including the mucosal wave[1]. Let $\mathbf{x}_i(t) = [x, y]$ denotes the position of i-th mesh vertex. The motion is defined as

$$\begin{aligned} x(t) &= x(\mathrm{t{=}0}) + A_i \sin(2\pi f_i t + \phi_i), \\ y(t) &= y(\mathrm{t{=}0}) + A_i \cos(2\pi f_i t + \phi_i), \end{aligned} \quad (3)$$

where the displacement of each vertex $\mathbf{x}_i$ is characterized by an amplitude A_i, frequency f_i, and phase shift ϕ_i.

In the present study, a single frequency $f_i = 100\,\mathrm{Hz}$ is prescribed for all vertices. The amplitude A_i varies piecewise linearly along the VF interface, while the phase ϕ_i is determined from experimentally measured mucosal wave propagation (kymographic data), cf. [3]. This parametrization enables realistic representation of the upward and lateral propagation of the mucosal wave.

2.3. Aeroacoustic model

Since the characteristic Mach number of the glottal flow is sufficiently low, the acoustic feedback on the flow field is negligible. Therefore, the aeroacoustic problem can be solved independently using a perturbation approach, where the incompressible flow solution acts solely as a source of sound. Here, we choose AWE approach for aeroacoustic modelling neglecting convective effects (justified in the low Mach number regime), see [5], for unknown acoustic pressure p^a

$$\frac{\partial^2 p^a}{\partial t^2} - c_0^2 \Delta p^a = -\frac{\partial^2 p'}{\partial t^2}, \quad (4)$$

where p' denotes hydrodynamic pressure fluctuations extracted from the incompressible flow simulation, which time derivatives represent the primar sound source here. This equation is solved in the whole acoustic domain Ω^a, while the source term on the right-hand side is nonzero only within the flow region Ω^f_{ref}.

On solid boundaries, acoustical sound hard (fully reflective) boundary conditions are imposed,

$$\frac{\partial p^a}{\partial \mathbf{n}} = 0, \quad (5)$$

where $\mathbf{n}$ denotes the outward unit normal to Ω^a. To prevent artificial reflections at the inlet and outlet, perfectly matched layers (PML) are employed.

3. Numerical Method

The proposed hybrid framework decomposes the fluid dynamics and acoustic propagation into two consecutive numerical problems. The incompressible flow is computed first, while the resulting hydrodynamic pressure fluctuations are subsequently employed as source terms for the acoustic simulation.

3.1. Flow simulation

The flow simulations are performed using the open-source finite-volume package OpenFOAM. Although the present contribution employs only prescribed vocal-fold motion, the computations are carried out within a general FSI framework developed by the au-

[1] The kinematic description is derived from the M5 model.

thors, where OpenFOAM is coupled with an in-house nonlinear finite-element solver through the preCICE coupling library [7]. In the present study the structural solver is omitted and the interface motion is prescribed directly, allowing efficient parallel computation while preserving the original mesh-motion strategy.
The governing equations are discretized by the finite volume method on polyhedral meshes with dynamic mesh motion based on the ALE formulation. Pressure–velocity coupling is performed using the PIMPLE algorithm. Time integration is performed using the first-order implicit Euler scheme with time step $\Delta t = 0.0001$s. Convective terms are approximated by bounded upwind discretization, whereas diffusive terms and gradients are evaluated using second-order Gauss linear schemes.

3.2. Coupling strategy

The hybrid computational workflow consists of four consecutive steps:

1. transient incompressible flow simulation in OpenFOAM,
2. extraction of the hydrodynamic pressure fluctuations and computation its time derivatives,
3. interpolation of the source term from the flow mesh onto the static acoustic mesh,
4. solution of the AWE in the acoustic domain.

The evaluation of $\frac{\partial^2 p'}{\partial t^2}$ is done on the fluid domain using central difference scheme. Then the conservative interpolation of sound sources from the CFD on the acoustic mesh is subsequently performed once per time step with the help of package openCFS, [8]. Since the acoustic problem is solved independently from the flow simulation, no feedback of the acoustic field to the flow is considered. The interpolation further permits the use of much coarser acoustic mesh than the flow mesh which leads to additional computational time reduction. In the current approach we omit effects of time-dependent acoustic domain, see [1].

3.3. Aeroacoustic simulation

The aeroacoustic wave equation (4) is discretized in space using conforming finite elements implemented in openCFS in the whole acoustic domain Ω^a, while the computed sound sources is used only on the right hand side in the domain Ω^a_{src} being a part of bigger Ω^a. Temporal discretization is performed by a second-order implicit time-integration scheme. PML technique is used in order to suppress unwanted artificial reflections at acoustically open boundaries.

4. Numerical Results

Simulations are performed for a symmetric glottal configuration with a prescribed vocal fold oscillation frequency of 100 Hz, corresponding to a typical phonation frequency. A uniform inlet velocity of $1.85\,\mathrm{m\,s^{-1}}$ is considered. After the initial transient, the flow reaches a periodic state and the subsequent 20 vibration cycles are evaluated, corresponding to a total simulated time of 0.2 s.

4.1. Airflow simulation

The airflow through the oscillating glottis forms a pulsating jet accompanied by strong pressure gradients and vortex shedding downstream of the constriction. These unsteady flow structures represent the primary sources of aerodynamic sound.
Two representative time instants are selected for detailed analysis. The first instant, $t = 0.1055$ s, corresponds to the phase of nearly complete glottal closure, while the second instant, $t = 0.1073$ s, is shortly after the glottis reaches its maximum opening, see also pressure signal measured at microphone B outside the mouth in Fig. 3.
Fig. 4 at $t = 0.1055$ s shows that the narrow glottal gap produces a significant pressure drop and only a weak jet develops downstream. The acoustic source terms are spread along decaying jet at supraglottal spaces, where the temporal pressure variations attain their highest values.
In contrast, Fig. 5 shows the flow field at $t = 0.1073, s$, shortly after the maximum glottal opening. At this stage, the glottal jet is rapidly accelerating into the supraglottal tract. The acoustic source term is concentrated primarily near the tip of the developing jet, where the strongest vortical structures are present.

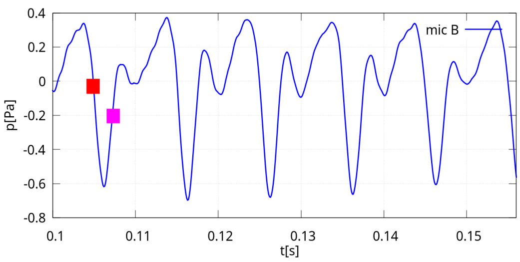

Figure 3: Pressure signal at microphone B outside the mouth. The red and purple markers indicate the time instants $t = 0.1055$ s and $t = 0.1073$ s analysed in Figs. 4 and 5.

4.2. Acoustic simulation

The acoustic pressure recorded at microphone B is analysed in the frequency domain. The resulting spectrum is shown in Fig. 6. As expected, the dominant spectral component corresponds to the prescribed vocal fold oscillation frequency of 100 Hz, while a sequence of higher harmonics is generated by the strongly nonlinear airflow through the oscillating glottis.
The frequency bands within ±50 Hz around the first three theoretical formants of the vowel [u:], located at 389 Hz, 987 Hz and 2299 Hz – see [9], are highlighted in Fig. 6. Although increased SPLs can be observed in these frequency bands, their amplitudes remain relatively small compared with the dominant harmonics

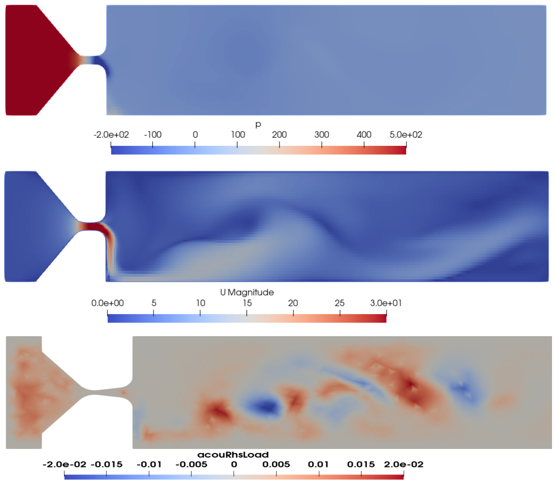

Figure 4: Pressure, velocity magnitude and interpolated acoustic source term at $t = 0.1055\,\mathrm{s}$.

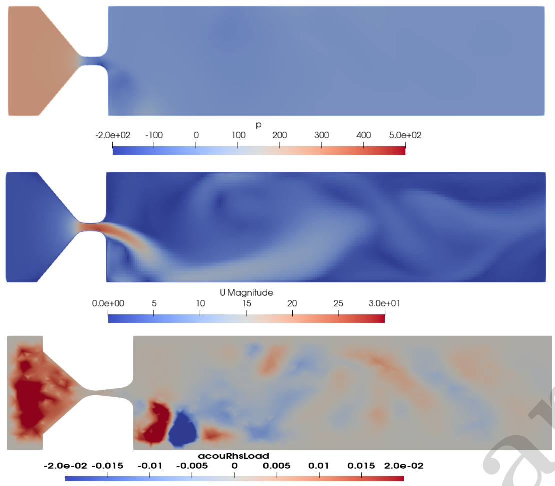

Figure 5: Pressure, velocity magnitude and interpolated acoustic source term at $t = 0.1073\,\mathrm{s}$.

associated with the prescribed vocal fold oscillation. The simulated spectrum exhibits the expected harmonic structure of voiced phonation together with indications of vocal tract resonance. In its current state, the proposed hybrid approach demonstrates the capability to couple aerodynamic sound generation with acoustic wave propagation in the vocal tract, providing a promising basis for future validation against experimental data and more realistic vocal fold models.

5. Conclusion

A hybrid computational framework for phonation based on prescribed vocal fold motion and the Acoustic Wave Equation (AWE) has been presented. Instead of fully coupled fluid–structure interaction, the prescribed vocal fold kinematics provide a simplified yet physically meaningful representation of the glottal dynamics. This approach allows controlled investigation of the aeroacoustic mechanisms involved in phonation

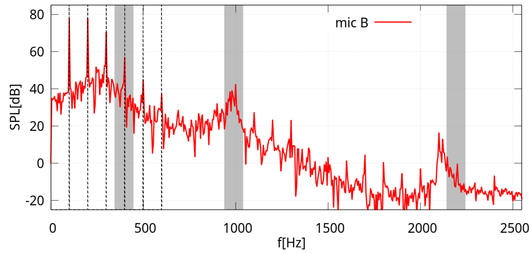

Figure 6: Power spectral density of the acoustic pressure at microphone B. Black vertical lines denote the first six harmonics of the prescribed vocal fold oscillation, while the gray shaded regions indicate the first three formants of the vowel [u:].

while avoiding numerical difficulties associated with vocal fold contact and strongly coupled fluid–structure interaction.

The numerical results demonstrate the formation of the glottal jet, the associated pressure drop across the glottis, and the resulting distribution of the acoustic source term. The computed acoustic spectra exhibit the expected harmonic structure and indicate the influence of vocal tract resonances.

Future work will focus on physiologically more representative vocal fold kinematics together incorporating more realistic vocal tract geometries. The proposed framework will be validated against experimental measurements, with the long-term objective of extending the current methodology to fully coupled fluid–structure–acoustic interaction simulations.

6. Acknowledgments

Authors thanks for support from Premium Academiae of Šárka Nečasová provided by the Czech Academy of Sciences as well as support provided by the Grant No. 25-15289K of Czech Science Foundation. Further support was provided by the Czech Technical University in Prague under the grants No. SGS24/120/OHK2/3T/12 and SGS25/123/OHK2/3T/12.

References

[1] S. Falk, S. Kniesburges, S. Schoder, *et al.*, "3D-FV-FE aeroacoustic larynx model for investigation of functional based voice disorders," *Frontiers in Physiology*, vol. 12, no. 616985, 2021. DOI: 10.3389/fphys.2021.616985.

[2] S. Zörner, P. Šidlof, A. Hüppe, and M. Kaltenbacher, "Flow and acoustic effects in the larynx for varying geometries," *Acta Acustica united with Acustica*, vol. 102, no. 2, pp. 257–267, 2016.

[3] P. S. Kumar and J. Švec, "Kinematic model for simulating mucosal wave phenomena on vocal folds," *Biomedical Signal Processing and Control*, 2018. DOI: 10.1016/J.BSPC.2018.12.002.

[4] R. C. Scherer, D. Shinwari, K. J. De Witt, C. Zhang, B. R. Kucinschi, and A. A. Afjeh, "Intraglottal pressure profiles for a symmetric and oblique glottis with a divergence angle of 10 degrees," *Journal of the Acoustical Society of America*, vol. 109, pp. 1616–1630, 2001.

[5] M. Kaltenbacher, S. Marburg, A. Beck, C.-D. Munz, U. Langer, and M. Neumüller, *Computational Acoustics*, M. Kaltenbacher, Ed. Springer, 2018, ISBN: 978-3-319-59037-0. DOI: 10.1007/978-3-319-59038-7.

[6] J. Valášek, P. Sváček, and J. Horáček, "On suitable inlet boundary conditions for fluid-structure interaction problems in a channel," *Applications of Mathematics*, vol. 64, no. 2, pp. 225–251, 2019. DOI: 10.21136/AM.2019.0267-18.

[7] P. Pučejdl and P. Sváček, "On numerical simulation of fluid-structure-interactions using preCICE for coupling of OpenFOAM with an in-house solver," in *Topical problems of fluid mechanics 2024*, 2024.

[8] S. Schoder and K. Roppert, "OpenCFS: Open source finite element software for coupled field simulation–part acoustics," *arXiv e-prints*, arXiv:2207.04443, 2022. DOI: 10.48550/arXiv.2207.04443.

[9] B. H. Story, I. R. Titze, and E. A. Hoffman, "Vocal tract area functions from magnetic resonance imaging," *The Journal of the Acoustical Society of America*, vol. 100, no. 1, pp. 537–554, 1996.